Title

Millisecond spatiotemporal dynamics of FRET biosensors by the pair correlation function and the phasor approach to FLIM

Journal

Proceedings of the National Academy of Sciences of the United States of America, 110(1)

ISSN

0027-8424

Authors

Hinde, Elizabeth

Digman, Michelle A

Hahn, Klaus M

et al.

Publication Date

2013-01-02

DOI

10.1073/pnas.1211882110

Millisecond spatiotemporal dynamics of FRET biosensors by the pair correlation function and the phasor approach to FLIM

Elizabeth Hinde[a], Michelle A. Digman[a,b], Klaus M. Hahn[c], and Enrico Gratton[a,b,1]

[a]Laboratory for Fluorescence Dynamics, Department of Biomedical Engineering, and [b]Department of Development and Cell Biology, University of California, Irvine, Irvine, CA 92617; and [c]Department of Pharmacology and Lineberger Cancer Center, University of North Carolina at Chapel Hill, Chapel Hill, NC 27599

Edited by Francisco Bezanilla, The University of Chicago, Chicago, IL, and approved November 13, 2012 (received for review July 11, 2012)

Here we present a fluctuation-based approach to biosensor Förster resonance energy transfer (FRET) detection that can measure the molecular flow and signaling activity of proteins in live cells. By simultaneous use of the phasor approach to fluorescence lifetime imaging microscopy (FLIM) and cross–pair correlation function (pCF) analysis along a line scanned in milliseconds, we detect the spatial localization of Rho GTPase activity (biosensor FRET signal) as well as the diffusive route adopted by this active population. In particular we find, for Rac1 and RhoA, distinct gradients of activation (FLIM-FRET) and a molecular flow pattern (pCF analysis) that explains the observed polarized GTPase activity. This multiplexed approach to biosensor FRET detection serves as a unique tool for dissection of the mechanism(s) by which key signaling proteins are spatially and temporally coordinated.

cellular diffusion | fluorescence correlation spectroscopy

To dissect the mechanism by which a signaling pathway is regulated it is necessary to not only measure the localization of the key signaling proteins, but also their activation at different subcellular locations. This is most often accomplished via the use of genetically encoded biosensors (1, 2). Given that the great majority of biosensor designs use a Förster resonance energy transfer (FRET) interaction as a report of the activity being probed, there is great interest in the development of methods for biosensor FRET detection with high spatial and temporal resolution (1). For example, in a recent study by Machacek and coworkers, the spatiotemporal coordination of several Rho GTPases was probed on the second and micrometer scale at the leading edge of migrating cells, via the use of a series of FRET biosensors (3). Edge velocity was correlated with the changing activation of GTPase biosensors in defined regions adjacent to the edge. This revealed correlations of RhoA, Rac1, and Cdc42 activity with leading-edge dynamics that had not previously been detected using static or low temporal resolution imaging. Along this line, in an even more recent study, Kunida et al. developed an image processing algorithm to extract the FRET values and velocities from an entire cell periphery (4). With this analytical approach they revealed several feedback regulations between Rac1 and membrane protrusion, which could not have been observed without use of a global field of view and high spatial resolution imaging (micrometer scale).

Determination of biosensor FRET in cells at a quantitative level is thought to be best achieved using the quenching of the donor lifetime, which directly detects the "on" and "off" state of the FRET biosensor. We recently demonstrated this property by applying the phasor approach to fluorescence lifetime imaging (FLIM) on the GTPase biosensors used by Machacek and coworkers (5). Using a frame mode acquisition we were able to spatially map and quantify the degree of Rac1 and RhoA activation in each pixel of an image as a function of time, independent of other sources of fluorescence for both single- and dual-chain designs. Lifetime-based methods of FRET detection are, however, limited by the intensity of the FRET signal, such that a frame mode acquisition can take many seconds to integrate sufficient counts per pixel. Thus, with this mode of acquisition we miss the transient localizations in Rac1 and RhoA activity previously observed by Machacek et al. Here we demonstrate that if FLIM data are instead acquired along a line scan, we gain sufficient temporal resolution to not only detect transient localizations in Rac1 and RhoA activation (FRET signal), but also to establish the diffusive route adopted by each Rho GTPase in the cell.

A FLIM line scan increases total pixel integration to an extent that enables a millisecond sampling frequency. Given that this timescale is comparable to the diffusive rate at which Rho GTPases traverse the cell upon activation (6), we have the opportunity to perform concomitant pair correlation function (pCF) analysis along the FLIM line scan and elucidate the molecular flow pattern adopted by each Rho family member upon activation. The pCF method is an approach to spatiotemporal correlation spectroscopy that maps the molecular flow pattern of a population of molecules along a line scan (7). From temporal cross-correlation of a pair of points at a given distance from each other, pCF analysis can define the diffusive route taken by molecules over many pixels (microns) along the line measured. In the case of a FRET experiment that employs a dual-chain biosensor, from cross–pair correlation function analysis of the donor molecules (Rho GTPase) with the acceptor molecules (affinity reagent) we can extract the diffusive route adopted by the active population of biosensor from the inactive population along a FLIM line scan.

From application of this multiplexed approach to biosensor FRET detection, we find for each Rho GTPase tested a distinct gradient of activation (based on FLIM-FRET data) and a molecular flow pattern (based on pCF analysis) that sheds light on observations of polarized GTPase activity. In particular we find that the mechanism by which Rac1 and RhoA are distributed throughout the cell during migration is highly organized in time and space, via a dynamic gradient of protein mobility that results in compartmentalized cascades of activation. Only by using a combination of FLIM-FRET and pair correlation function analysis, do we have the opportunity to simultaneously measure and quantify the molecular flow and the signaling activity of proteins in live cells. Thus, as demonstrated here on Rho GTPases, this multiplexed approach to biosensor FRET detection serves as a unique tool for dissection of the mechanism(s) by which the key proteins in a given signaling pathway are spatially and temporally coordinated. Furthermore, given that the diffusive motion of proteins and their binding-dissociation reactions with cellular organelles is critical to several different cell functions, we believe the ability of this method to distinguish the different conformational states of a population of molecules while simultaneously following their independent molecular paths makes this analytical tool invaluable to cell biologists in general.

Author contributions: E.H. and E.G. designed research; E.H. performed research; M.A.D. and K.M.H. contributed new reagents/analytic tools; E.H., M.A.D., and E.G. analyzed data; and E.H. wrote the paper.

The authors declare no conflict of interest.

This article is a PNAS Direct Submission.

Freely available online through the PNAS open access option.

[1]To whom correspondence should be addressed. E-mail: egratton22@yahoo.com.

This article contains supporting information online at www.pnas.org/lookup/suppl/doi:10.1073/pnas.1211882110/-/DCSupplemental.

Results

Measuring Biosensor Activation: FLIM-FRET Analysis of Rac1 Along a Line Scan. We measure concomitantly the intensity and lifetime of the Rac1 dual-chain biosensor in the donor (Rac1-CyPet) and acceptor (PBD-Ypet) channel along a line that extends from the front to the rear of a migrating cell. We rapidly scan this line in time following the experimental setup specified in *Materials and Methods* to obtain at each pixel position along the line an intensity fluctuation, as well as a time series of the phasor coordinates that describe the pixel lifetime. We acquire a FLIM line scan before epidermal growth factor (EGF) stimulation and then two to three line scans afterward, each separated by 3 min. With each line scan we monitor, with millisecond resolution, variations in Rac1 activity (lifetime) and mobility (intensity fluctuation) along the line. In between the FLIM line-scan measurements we acquire FLIM frame acquisitions of the whole cell (which take ~30 s) to establish the direction of cell migration and the distribution of overall Rac1 activity. For each line experiment acquired we first analyze the lifetime signal from the donor channel and determine the spatial distribution of FRET as a function of time, based on the degree of quenching of the donor lifetime. From this analysis we gain insight into when and where Rac1 is active, which ultimately informs interpretation of the pair correlation function analysis (Rac1 mobility).

As can be seen from the intensity images in Fig. 1*A* the selected NIH 3T3 cell shows a morphology and incremental change in position, which indicates cell migration to be from upper left to lower right. The FLIM images derived from each frame acquisition (Fig. 1*B*) show increasing Rac1 activation across the entire cell after EGF stimulation. The intensity of Rac1-Cypet (donor channel) measured along the FLIM line scan that traverses the axis of the cell (Fig. 1*C*) shows, before EGF stimulation, a high Rac1 localization at the back of the cell that is heterogeneous in distribution, due to a significant accumulation of Rac1 molecules in discrete positions along the line. With increasing time after EGF stimulation the distribution of Rac1 activation is shown to be pushed toward the front of the cell, with Rac1 forming a more gradual concentration gradient that remains heterogeneous in distribution, but with the discrete locations of Rac1 accumulation more regularly spaced across the entire cell length. If we analyze the lifetime of Rac1-Cypet (donor channel) along this same line scan (Fig. 1*D*) we obtain a phasor distribution (Fig. 1*E*) that extends from the unquenched donor lifetime toward shorter lifetimes indicative of FRET (Rac1 activity). By pseudocoloring the FLIM line scan (Fig. 1*D*) with a palette that extends from the donor phasor toward the FRET state (defined in Fig. 1*E*) we see that before EGF stimulation there is no detectable gradient of Rac1 activity from the back to the front of the cell. Immediately after stimulation, however, we see a gradient of activation generated along the line scan (Fig. 1*E*). If we extract from the FLIM line scan the tau-phase coordinate (see Fig. 1*C* for the definition of tau-phase) of the first and last 10 columns as a function of time (Fig. 1*F*), we see that the front of the cell is activated first at 180 s (0 s after stimulation) followed by a gradual activation of the back of the cell over the next 2 min (180–360 s). The temporal and spatial profile of Rac1 activation revealed by FRET analysis of the FLIM line scan was observed in eight cells with some variation in the degree and timing of activation (as shown in Fig. S1). The front-to-back order of activation, however, was maintained in all of the measured NIH 3T3 cells, a result that is in agreement with Machacek and coworkers (3).

Measuring Biosensor Molecular Flow: pCF Analysis of Rac1 Along a FLIM Line Scan. With this spatial and temporal profile of Rac1 activation determined by the FLIM analysis, we then perform pair correlation analysis for each intensity fluctuation acquired along the FLIM line scan (Fig. 2*A*), using a pixel distance that tests flow every 0.5–1 μm (pCF(5–10)) initially in the donor channel alone (Rac1-CyPet). Pair correlation analysis was performed within this range of pixel distance because a spatiotemporally organized population of molecules was extracted. This is a phenomenon related to Rac1 regulation because concomitant pair correlation analysis of a cell cotransfected with free mCherry under the same experimental conditions produces a random pattern of correlation for all pCF distances due to unregulated motion. Given the complexity of the pair correlation carpets derived, we have superimposed a scatterplot of the average time Rac1 takes to flow 1 μm by averaging the pair correlation profile derived every 10 columns and plotting the maxima (for every 40 columns). From this analysis in the left-to-right direction we find before EGF stimulation (Fig. 2*B*), Rac1-Cypet flow from discrete positions along the line with

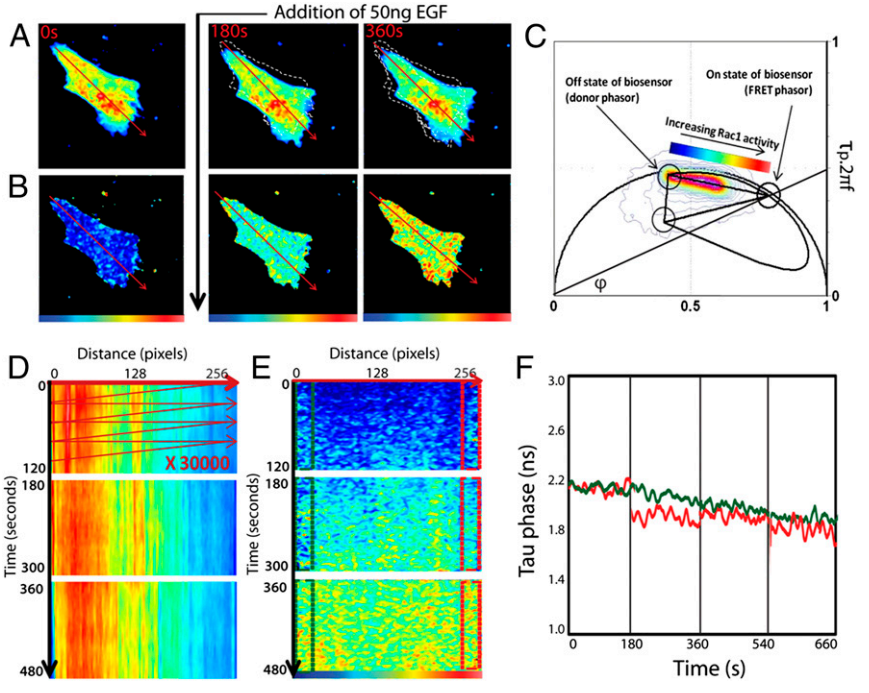

Fig. 1. Rac1 activation (FLIM-FRET analysis). (*A*) Intensity images before and after EGF stimulation (donor channel) show the cell to move from the top left to the bottom right of the frame, as indicated by the superimposed outline of the cell position (dashed white line) of the previous time point(s). (*B*) FLIM images of the FRET experiment colored according to the palette defined in *C*, which ranges from blue to red with an increase in Rac1 activity. (*C*) Phasor distribution of lifetimes measured for the Rac biosensor experiment depicted in *A* and *B*, with the theoretical FRET trajectory superimposed (black line) to determine the biosensor FRET efficiency. The lifetime of a given molecular species can be calculated from the phase shift (δ), by extrapolation of the phasor vector to the left-hand axis, which is linearly related to tau phase for a given angular frequency ($2\pi f$*tau-phase). (*D*) Intensity carpet of Rac1-Cypet across the axis of the cell, which is a construction of the 30,000 lines measured along the line drawn in *A*, as a function of time. (*E*) Tau-phase carpet of Rac1-Cypet activity across the axis of the cell. (*F*) Average lifetime of the first 10 columns of the line scan (back of the cell) and the last 10 columns of the line scan (front of the cell) show that after EGF stimulation, the tau-phase recorded at the front of the cell is reduced from 2.2 to 2ns at 180s, which indicates quenching of the donor lifetime and therefore early activation of Rac1 at the front of the cell. With increasing time after stimulation we see the back of the cell gradually becoming active, as indicated by a gradual decrease in tau-phase from 2.2 to 2ns from 180 to 360s.

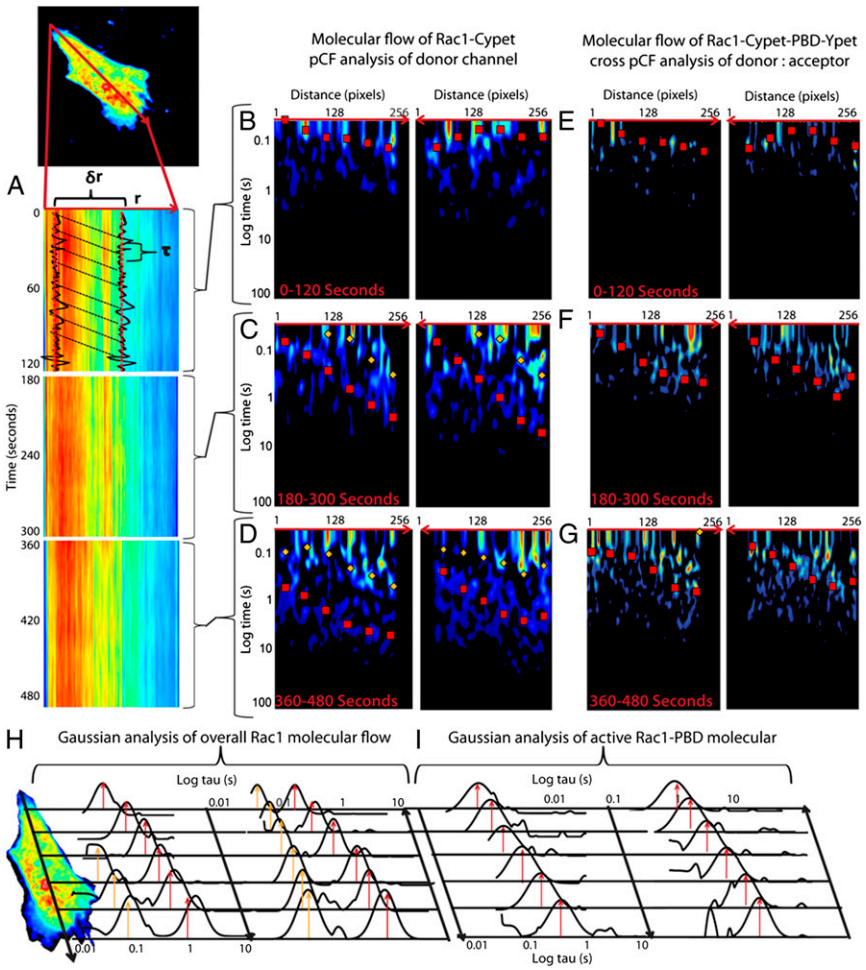

Fig. 2. Rac1 molecular flow (pCF analysis). (*A*) Intensity carpet of the line scan acquired along the axis of the migrating cell in Fig. 1, cut into 3-min intervals for pCF analysis. We cross-correlate the intensity fluctuations that originate from each pixel position along the line scan with another intensity fluctuation δr pixels away (where $\delta r = 10$ pixels ~1 μm) for all possible delay times (represented here as τ), to establish the characteristic time taken for Rac1 molecules to flow across the line scan. (*B–D*) pCF of the FLIM line scan in the donor channel (Rac1-Cypet) from left to right and then right to left at a distance of 1 μm for the first time segment of the intensity carpet (0–120 s), the second time segment of the intensity carpet (180–300 s), and the third time segment of the intensity carpet (360–480 s). The analysis presented in *B–D* detects molecular flow of both active and inactive Rac1. To extract the active population of Rac1 we must cross-correlate the donor channel (Rac1-Cypet) with the acceptor channel (PBD-Ypet). Thus, in *E–G* we perform cross-pCF analysis of the line scan in the donor channel with the acceptor channel from left to right and then right to left at a distance of 1 μm for the first time segment of the intensity carpet (0–120 s), the second time segment of the intensity carpet (180–300 s), and the third time segment of the intensity carpet (360–480 s). (*H*) Gaussian analysis of pair correlation carpets derived in *D*, which measure overall Rac1-CYpet flow from left to right and right to left. (*I*) Gaussian analysis of pair correlation carpets, which measures active Rac1-CyPet-PBD-Ypet flow from left to right and right to left.

a characteristic (end to end) time of 0.1 s. If we reverse the direction of analysis to measure flow from right to left, we also see Rac1-Cypet flow from discrete locations along the line with a characteristic time of 0.1 s. Thus, before stimulation, Rac1-Cypet flow is bidirectional and occurs with a characteristic time that is independent of position along the line.

Immediately after EGF stimulation in Fig. 2*D*, we see from left to right that the time taken for Rac1 to flow a distance of 1 μm increases as a function of position along the line (from back to front) and that for each position, there are two timescales upon which this trend occurs. In particular, there is a gradient of Rac1 mobility that extends from the back to the front of the cell, as indicated by peaks of positive correlation at increasing time delays that range from 0.2 to 10 s, respectively (red data series). For the same pixel positions along the line, an additional family of correlations that is spatially offset by 5 μm with respect to the back of the cell is observed. These peaks of positive correlation represent a second and faster gradient of Rac1 mobility that ranges from 0.05 to 0.8 s, depending on the position along the cell (yellow data series). If we then perform pair correlation function analysis in the reverse direction from right to left, at this time (3 min) we see the same complex but organized pattern of mobility that was observed for left-to-right flow. That is, Rac1-Cypet mobility from the front to the back of the cell occurs with a characteristic time that decreases along the cell axis and there are two timescales upon which this trend is observed. As can be seen in Fig. 2*E*, with increasing time after EGF stimulation (6 min) the key features of this complex pattern of mobility are maintained.

Together these results indicate Rac1 flow between the front and rear of a motile cell to be governed by a bidirectional mechanism that enables a cascaded timing. The overall pattern of Rac1-Cypet molecular flow measured by pair correlation analysis can more clearly be observed by a Gaussian analysis of the average pair correlation profiles derived every 10 columns in Fig. 2 *B–D*. That is, if we convolute the average pCF profile calculated for each 10 columns with a Gaussian profile, we obtained a simplified temporal profile of the molecular flow occurring at each consecutive location along the line scan. In Fig. 2*H* we perform this analysis for the pair correlation carpets presented in Fig. 2*D* and, as can be seen, extract the major components of overall Rac1 molecular flow. Mobility from the back to the front of the cell decreases along the cell axis, there are two timescales upon which this trend is observed (indicated by the yellow and red scatterplots), and the same is true in the reverse direction. The two gradients of reduced Rac1 mobility from the back to the front of the cell, observed after EGF stimulation, were observed in eight cells with variation in the timing and positioning of the individual peaks of positive correlation (Fig. S2). By analyzing the molecular flow of Rac1-Cypet alone, however, we cannot attribute this behavior to the diffusive dynamics of Rac1 activation because we also detect molecular flow from inactive Rac1.

To extract the diffusive dynamics of the active population of Rac1 (membrane bound) from the inactive population of molecules (cytosolic pool) we need to cross-correlate the molecular flow of Rac1-Cypet (donor channel) with the molecular flow of its active binding partner PBD-Ypet (acceptor channel). The PBD-Ypet will bind only to the activated form of the GTPase (3, 8). Fig. 2 *F* and *H* shows this analysis for each time segment presented in Fig. 2 *C–E*, respectively. Cross–pair correlation analysis was performed at a distance that tests flow of Rac1-Cypet-PBD-Ypet every 1 μm and, as can be seen from this analysis, several bands of correlation that were previously observed disappear. The pattern of correlation that remains represents the molecular flow of the

active Rac1 population (membrane bound), a single gradient of mobility that extends across the axis of the cell and, in general, temporally corresponds to the slower family of correlation that was observed with pair correlation analysis of Rac1-Cypet alone (indicated by red data series in Fig. 2*H*). Thus, the faster family of correlation previously observed in Fig. 2 *B–D* (indicated by yellow data series) must represent the inactive cytosolic pool of Rac1. Again we see this result more clearly in Fig. 2*I* from Gaussian analysis of the average cross–pair correlation profiles derived in Fig. 2*G*. That is, the molecular flow of Rac1-Cypet-PBD-Ypet is reduced to a single gradient of mobility that represents the longer timescale gradient of flow measured in Fig. 2*H*, and that this gradient is maintained in the reverse direction.

RhoA Spatiotemporal Dynamics by FLIM-FRET and pCF Analysis. If we apply the same experimental procedure and analytical approach used to characterize Rac1 spatiotemporal dynamics to RhoA we find a very different mode of regulation in terms of both biosensor activation and molecular flow. As can be seen from Fig. 3 *A* and *B*, the selected cell shows a morphology and incremental change in position that indicate cell migration to be from lower left to upper right with increasing RhoA activation after lysophosphatidic acid (LPA) stimulation. The intensity of RhoA-Cypet (donor channel) measured along the FLIM line scan that was drawn from the front to the back of the cell (Fig. 3*C*) shows a slight concentration gradient from front to back that is highly heterogeneous in distribution due to accumulation in discrete locations. With increasing time after LPA stimulation, we see this localization become excluded from the nuclear region and with even more discrete points of accumulation at the front and back of the cell. If we then analyze the lifetime component of the FLIM line scan in the donor channel (Fig. 3*D*) and pseudocolor it with a palette that extends from the donor phasor toward the FRET state (Fig. 3*E*), we see that before LPA stimulation there is no detectable RhoA activity from the back to the front of the cell. By the first time point acquired after stimulation, however, we see a wave of activation that is first observed at the back of the cell and propagates along the line scan toward the front. In particular if we extract from the FLIM line scan the tau-phase coordinate of the first and last 10 columns along the line scan as a function of time (Fig. 3*F*), we see that at 3 min, both the back and front of cell become activated to different extents, with the back initially being more active than the front. At 6 min, however, we see RhoA activity at the back of the cell reduced, as indicated by an increase in tau-phase, with a simultaneous increase in activity at the front of the cell, which yields an equivalent degree of activation. The temporal and spatial profile of RhoA activation revealed by FRET analysis of the FLIM line scan was observed in eight cells with some variation in the degree and timing of activation (Fig. S3). The back-to-front order of activation, however, was maintained in all of the measured NIH 3T3 cells, a result that is in agreement with Machacek et al. (3).

With this spatiotemporal pattern of RhoA activation in mind we then performed pair correlation analysis along the FLIM line scan (Fig. 4*A*) and found that, similarly to Rac1, RhoA molecular flow before growth factor stimulation with LPA is bidirectional and occurs with a characteristic time of 0.1 s, independent of position along the line. Immediately after stimulation, however, we see a molecular flow pattern that is markedly different from that observed for Rac1. As can be seen in Fig. 4*C* from left to right we see a significant increase in the time taken for RhoA to flow 1 μm at the very back of the cell (10 s) compared with the rest of the cell, where the time taken to flow this same distance remains the same as before stimulation (0.1 s) (red data series). If we perform pair correlation function analysis in the reverse direction from right to left at this time (3 min), we see a significant increase in the time taken to flow 1 μm from the very front of the cell backward (10 s) compared with the rest of the cell where it takes 0.1 s to flow this same distance (red data series). Together these results indicate a direction-dependent mechanism that holds RhoA at the very back and front of the cell 100 times longer than everywhere else in the cell; this is in contrast to Rac1, which was governed by a bidirectional mechanism.

With more time after LPA stimulation (at 6 min), we see that flow from the back of the cell is maintained at 10 s, but now with a cascaded gradient of RhoA mobility that extends from this location toward the front of the cell. That is, the time taken for RhoA to flow a distance of 1 μm decreases on two timescales, a slow gradient from 10 to 1 s (red data series) and a faster gradient from 1 to 0.1 s (yellow data series). If we perform pair correlation function analysis in the reverse direction from right to left at this time (6 min), we again see a cascaded gradient of RhoA flow but with an opposing temporal trend. That is, from right to left we see two families of positive correlation, which

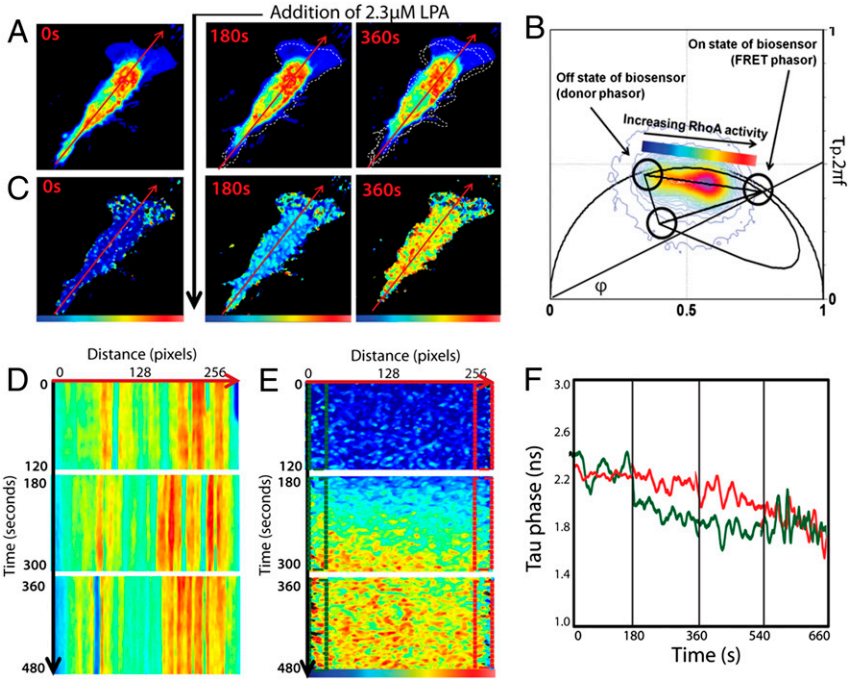

Fig. 3. RhoA activation (FLIM-FRET analysis). (*A*) Intensity images before and after LPA stimulation (donor channel) show the cell to change position from the bottom left-hand corner toward the top right-hand corner. (*B*) FLIM images of the FRET experiment colored according to the palette defined in *C*, which ranges from blue to red with an increase in RhoA activity. (*C*) Phasor distribution of lifetimes measured for the RhoA biosensor experiment depicted in *A* and *B*, with the theoretical FRET trajectory superimposed (black line) to determine the biosensor FRET efficiency. (*D*) Intensity carpet of RhoA-Cypet across the axis of the cell. (*E*) Tau-phase carpet of RhoA-Cypet activity across the axis of the cell. (*F*) Average lifetime of the first 10 columns of the line scan (back of the cell) and the last 10 columns of the line scan (front of the cell) show that after LPA stimulation, the tau-phase recorded at the back and front of the cell gradually reduce from 2.0 to 1.6 ns, with the back of the cell reaching 1.6 ns, at a faster rate than the front of the cell.

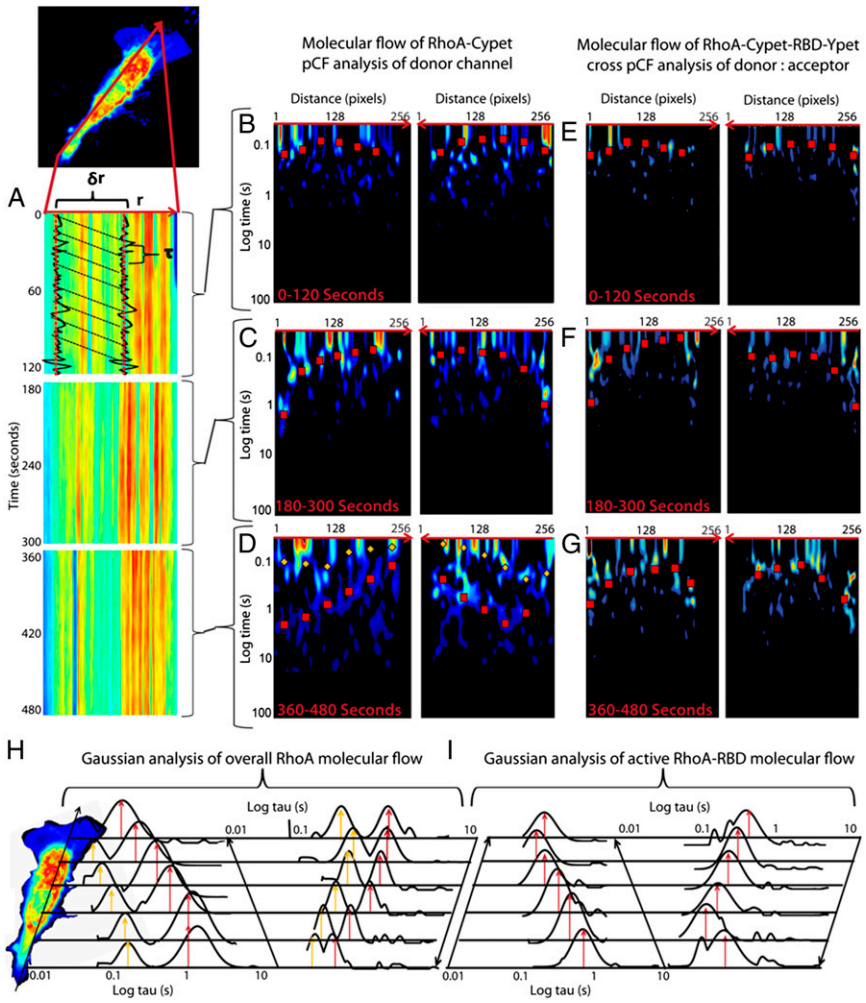

Fig. 4. RhoA molecular flow (pCF analysis). (*A*) Intensity carpet of the line scan acquired along the front–back axis of the migrating cell in Fig. 3, cut into 3-min intervals for pCF analysis. (*B–D*) pCF of the line scan in the donor channel (RhoA-Cypet) from left to right and then right to left at a distance of 1 μm for the first time segment of the intensity carpet (0–120 s), the second time segment of the intensity carpet (180–300 s), and the third time segment of the intensity carpet (360–480 s). With this analysis molecular flow of active and inactive RhoA is detected. To extract the active population of RhoA we must cross-correlate the donor channel (RhoA-Cypet) with the acceptor channel (RBD-Ypet). (*E–G*) Cross-pCF analysis of the FLIM line scan in the donor channel with the acceptor channel from left to right and then right to left at a distance of 1 um for the first time segment of the intensity carpet (0–120 s), the second time segment of the intensity carpet (180–300 s), and the third time segment of the intensity carpet (360–480 s). (*H*) Gaussian analysis of pair correlation carpets derived in (*D*), which measure overall RhoA-CYpet flow from left to right and right to left. (*I*) Gaussian analysis of pair correlation carpets, which measure active RhoA-CyPet-RBD-Ypet flow from left to right and right to left.

indicate a decrease in the time taken to flow 1 μm from the front to the back of the cell on two timescales; a slow gradient from 10 to 1 s (red data series) and a faster gradient from 1 to 0.1 s (yellow data series). Together these results indicate RhoA flow across the cell to be governed by a direction-dependent mechanism that distributes the protein at either end of the cell, with a cascaded timing. This phenomenon is related to RhoA regulation, because concomitant pair correlation analysis of a cell cotransfected with free mCherry under the same experimental conditions produces a random pattern of correlation for all pCF distances, due to unregulated motion. This direction-dependent gradient of flow, which is more clearly shown in Fig. 4*H* by Gaussian analysis of the average pair correlation profiles derived in Fig. 4*D*, was observed in eight cells, with variation in the timing and positioning of the individual peaks of positive correlation (Fig. S4). We then performed the cross–pair correlation analysis between RhoA-CyPet (donor channel) and its binding partner RBD-Ypet to extract the diffusive dynamics of the active population of RhoA. Fig. 4 *F* and *H* shows this analysis for each time segment presented in Fig. 4 *C–E* respectively, and as can be seen, similarly to Rac1, the fast gradient of correlation previously observed from pair correlation analysis of RhoA-Cypet alone disappears. Again from Gaussian analysis of the pair correlation carpets derived in Fig. 4*E* this result is clearly observed.

Discussion

From combining the phasor approach to biosensor FRET detection with pair correlation function (pCF) analysis along a line-scan acquisition, we find for each Rho GTPase tested a distinct gradient of activation (based on FLIM data) and a molecular flow pattern (based on pCF analysis) that explains the observed polarized GTPase activity. In particular, we find that the mechanism by which Rac1 and RhoA are distributed upon cell migration is highly organized in time and space, resulting in dynamic gradients of protein mobility that change during cell migration and yield compartmentalized cascades of activation. Reverse pair correlation analysis along the line scan found that the gradients of mobility established in Rac1 were bidirectional; whereas, in contrast, RhoA gradients were in opposition, resulting in an accumulation of protein at either end of the cell. We propose the concept that the cascaded gradients of GTPase mobility that we observe in migrating cells serve as a mechanism that dynamically distributes GTPase activity with specific subcellular localization.

Rac1 and RhoA are critical regulators of cell polarity in many cell types (9). They play opposing roles at the front and rear of the cell; Rac1 induces cell protrusion via the Arp2/3 complex and is therefore activated selectively at the cell front (10). In contrast, RhoA has been shown to mediate contraction at the rear of the cell, while also driving actin-mediated protrusion at the cell front via formin activation (9). The mechanisms by which Rac1 and RhoA activities are restricted to specific regions remain unknown; pCF/FLIM indicates that regulation of subcellular flow can play an important role. RhoA activation may be restricted to the rear via the observed asymmetric flow; although in contrast Rac1, which moved equally well in all directions, is likely activated locally via spatial control of upstream signals. Previous work has suggested that actin and other cytoskeletal components form barriers to diffusion and accelerate cross-cell transport by restricting trafficking to particular pathways (11). pCF/ FLIM makes these pathways

visible and will enable us to correlate localized activation with directed movement through specific subcellular regions.

By cross–pair correlation function analysis of the molecular flow of the donor channel (Rac1 or RhoA) with the molecular flow of its active binding partner in the acceptor channel, we were able to track the diffusive dynamics of the active population of GTPase (membrane bound) as well as quantify the degree of activation by FLIM analysis of the FRET signal. Only with this multiplexed approach do we have the opportunity to simultaneously measure and quantify the molecular flow and signaling activity of proteins in live cells. The FLIM line scan is a method of acquisition that, by enabling concomitant fluctuation analysis, serves as a unique tool for dissection of the mechanism(s) by which key signaling proteins are spatially and temporally coordinated. As demonstrated here for Rac1 and RhoA, we anticipate that application of this method to other key proteins will result in fundamental advances toward understanding the intracellular mechanisms of spatiotemporal regulation.

Materials and Methods

Cell Culture and Treatments. NIH 3T3 cells were grown in high-glucose medium from Invitrogen, supplemented with 10% (vol/vol) FBS, 5 mL of Pen-Strep and Hepes at 37 °C and in 5% CO_2. Freshly split cells were plated onto 35-mm glass-bottom dishes coated with fibronectin and then, after 24 h, transiently transfected with the following series of GTPase biosensors sourced from the Hahn Lab, University of North Carolina (www.hahnlab.com): (*i*) Rac1 FLARE dual-chain biosensor (CyPet-Rac1 and YPet-PBD) and (*ii*) RhoA FLARE dual chain biosensor (CyPet-RhoA and YPet-RBD). The plated cells were then left for an additional 24 h at 37 °C/5% CO_2 and then serum starved in unsupplemented high-glucose medium for 4 h. The Rac biosensors tested were stimulated with 50 ng/ml EGF (Sigma Aldrich). The Rho biosensors tested were stimulated with 2.3 μM of LPA (Sigma Aldrich).

Microscope. FLIM and pair correlation function data were acquired concomitantly with the Zeiss LSM710 META laser scanning microscope, coupled to a two-photon Ti:Sapphire laser (Spectra-Physics) and an ISS A320 FastFLIM box to acquire the lifetime data. A 40× water immersion objective 1.2 N.A. (Zeiss) was used for all experiments. The donor fluorophore of each biosensor was excited at 800 nm: this wavelength caused negligible direct excitation of the acceptor fluorophore. A SP 760-nm dichroic filter was used to separate the fluorescence signal from the laser light. The fluorescence signal was directed through a 509 LP CFP/YFP filter, and the donor and acceptor signal split between two photomultiplier detectors (H7422P-40; Hamamatsu), with the following bandwidth filters in front of each: CFP 470/22 and YFP 542/27, respectively.

We simultaneously acquire intensity and lifetime data by rapidly scanning a two-photon Ti:Sapphire laser beam (800 nm) along a line drawn across the axis of a migrating cell; the line length varied between 24 and 30 μm depending on the selected cell. The line pixel size was set to 256, which gave a pixel size of ∼0.1 μm. The scanning speed was set at 25.61 μs/pixel, which resulted in a line time of 15 ms. For each FLIM line-scan experiment 15,000 lines were acquired. Together these conditions resulted in an acquisition time of ∼2 min. Calibration of the system and phasor plot space was performed by measuring fluorescein (pH 9.0), which has a known single exponential lifetime of 4.04 ns. The FLIM and pair correlation function data were acquired and processed by the SimFCS software developed at the Laboratory for Fluorescence Dynamics (www.lfd.uci.edu).

FLIM-FRET Data Analysis. ***Phasor transformation.*** The phasor transformation and data analysis were performed using the SimFCS software available at the www.lfd.uci.edu, as described in previously published papers (5, 12). In brief, the fluorescence decay in each pixel of the FLIM line scan is transformed into the sine and cosine components, which are then represented in a 2D polar plot (phasor plot), according to the equations defined in (12). Each pixel of the FLIM line scan gives rise to a single point (phasor) in the phasor plot, and when used in reciprocal mode, enables each point of the phasor plot to be mapped to each pixel of the FLIM line scan. Because phasors follow simple vector algebra, it is possible to determine the fractional contribution of two or more independent molecular species coexisting in the same pixel. Thus, in the case of two independent species, all possible weightings give a phasor distribution along a linear trajectory that joins the phasors of the individual species in pure form (12).

In the case of an FRET experiment where the lifetime of the donor molecule is changed upon interaction with an acceptor molecule, the realization of all possible phasors quenched with different efficiencies describe a curved trajectory in the phasor plot (5). The experimental position of the phasor of a given pixel along the trajectory determines the amount of quenching and therefore the FRET efficiency of that location. The contributions of the background and of the donor without acceptor are evaluated using the rule of the linear combination, with the background phasor and the donor unquenched determined independently. In the case of a dual-chain biosensor, which has a fixed FRET efficiency, the linear combination of phasor clusters between the donor phasor and FRET state of the biosensor represent the varying contributions of donor fluorescence and quenched donor fluorescence in any one pixel. By moving the phasor cursor along the straight line drawn between these two terminal phasor locations, we can calculate the exact fractional contribution of quenched donor fluorescence for each pixel highlighted (5).

Pair correlation function analysis. Calculation of the pair correlation functions was done using the SimFCS software developed at the Laboratory for Fluorescence Dynamics (www.lfd.uci.edu). Details about the mathematical derivation of the pCF for diffusing particles can be found in previously published papers (7, 13, 14). For the experiments reported here the distance between adjacent pixels is ∼0.1 μm. We performed all pair correlation analysis at a distance of 5–10 pixels [i.e., *pCF(10)*], which means that the correlation function was calculated along the line every 0.5–1 μm. We use the maximum of the *pCF(n)* to determine the average time a molecule takes to travel a given distance. This time will change depending on the obstacles or barriers to diffusion encountered by the molecules along the line of measurement.

Given that the line-scan experiments performed were positioned across cells stimulated to migrate, whole-cell movement during line-scan acquisition was found to cause major artifact upon pair correlation function analysis of Rho GTPase molecular dynamics, by introduction of very slow and large amplitude correlations. Because we were not interested in whole-cell movement, which occurs on a much longer timescale than Rho GTPase diffusion (active and inactive), we first detrend each line scan by application of a moving average (every 1,000 lines ∼15 s), which corrects for whole-cell movement without detracting from the fluctuation dynamics due to Rac1 or RhoA diffusion, before pair correlation analysis.

Gaussian analysis. Gaussian analysis of the pair correlation carpets derived in Figs. 2 and 4 was done using the SimFCS software developed at the Laboratory for Fluorescence Dynamics (www.lfd.uci.edu). In general we averaged every 10 columns along a derived pair correlation carpet and then convoluted the average pCF profile calculated for each 10 columns with a Gaussian profile, to obtain a simplified temporal profile of the molecular flow occurring at each consecutive location along the line scan. We then extracted the profile and plotted as a function of position along the line scan.

ACKNOWLEDGMENTS. We thank Milka Stakic for cultivating and transfecting the cells. This work is supported in part by Grants NIH-P41 P41-RRO3155 (to E.G. and M.A.D.), NIH-P50-GM076516 (to E.G. and E.H.), Cell Migration Consortium Grants U54 GM064346 (to E.G. and M.A.D.), GM090317 (to K.M.H.), and GM057464 (to K.M.H).

1. Welch CM, Elliott H, Danuser G, Hahn KM (2011) Imaging the coordination of multiple signalling activities in living cells. *Nat Rev Mol Cell Biol* 12(11):749–756.
2. Hodgson L, Shen F, Hahn K (2010) Biosensors for characterizing the dynamics of rho family GTPases in living cells. *Curr Protoc Cell Biol* 14(11):11–26.
3. Machacek M, et al. (2009) Coordination of Rho GTPase activities during cell protrusion. *Nature* 461(7260):99–103.
4. Kunida K, Matsuda M, Aoki K (2012) FRET imaging and statistical signal processing reveal positive and negative feedback loops regulating the morphology of randomly migrating HT-1080 cells. *J Cell Sci* 125(10):2381–2392.
5. Hinde E, Digman MA, Welch C, Hahn KM, Gratton E (2012) Biosensor Forster resonance energy transfer detection by the phasor approach to fluorescence lifetime imaging microscopy. *Microsc Res Tech* 75(3):271–281.
6. Moissoglu K, Slepchenko BM, Meller N, Horwitz AF, Schwartz MA (2006) In vivo dynamics of Rac-membrane interactions. *Mol Biol Cell* 17(6):2770–2779.
7. Digman MA, Gratton E (2009) Imaging barriers to diffusion by pair correlation functions. *Biophys J* 97(2):665–673.
8. Kraynov VS, et al. (2000) Localized Rac activation dynamics visualized in living cells. *Science* 290(5490):333–337.
9. Hall A (2005) Rho GTPases and the control of cell behaviour. *Biochem Soc Trans* 33(5):891–895.
10. Weiss M, Nilsson T (2004) In a mirror dimly: Tracing the movements of molecules in living cells. *Trends Cell Biol* 14(5):267–273.
11. Katsuki T, Joshi R, Ailani D, Hiromi Y (2011) Compartmentalization within neurites: Its mechanisms and implications. *Dev Neurobiol* 71(6):458–473.
12. Digman MA, Caiolfa VR, Zamai M, Gratton E (2008) The phasor approach to fluorescence lifetime imaging analysis. *Biophys J* 94(2):L14–L16.
13. Cardarelli F, Gratton E (2010) In vivo imaging of single-molecule translocation through nuclear pore complexes by pair correlation functions. *PLoS ONE* 5(5):e10475.
14. Hinde E, Cardarelli F, Digman MA, Gratton E (2010) In vivo pair correlation analysis of EGFP intranuclear diffusion reveals DNA-dependent molecular flow. *Proc Natl Acad Sci USA* 107(38):16560–16565.